



# Understanding the hydrological performance of green and grey roofs during winter in cold climate regions

Noëlie Maurin<sup>a,\*</sup>, Elhadi H.M. Abdalla<sup>a</sup>, Tone Merete Muthanna<sup>b</sup>, Edvard Sivertsen<sup>a</sup>

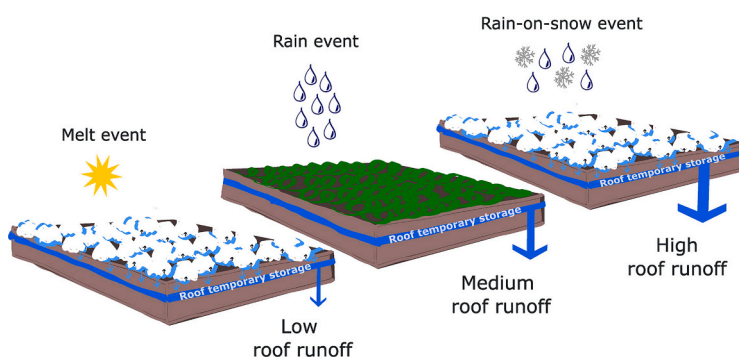
<sup>a</sup> SINTEF Community, Infrastructure, S.P. Andersens veg 3, 7031 Trondheim, Norway

<sup>b</sup> Norwegian University of Science and Technology, Civil and Environmental Engineering, S.P. Andersens veg 5, 7031 Trondheim, Norway

## HIGHLIGHTS

- A snow model was found suitable for modelling snow melt of green and grey roofs.
- Developed a method to separate winter events into rain, melt and rain-on-snow events
- Rain-on-snow events have the longest duration and yield highest peak runoff.
- Green and grey roofs can manage rain-on-snow if designed properly.

## GRAPHICAL ABSTRACT



## ARTICLE INFO

Editor: Ashantha Goonetilleke

### Keywords:

Stormwater management  
Green infrastructure  
Winter events  
Rain-on snow  
Melt  
HBV model

## ABSTRACT

Green and grey roofs have emerged as promising and sustainable measures for effectively managing stormwater in urban catchments. However, there is a gap in the literature in understanding and modelling the hydrological performance of these roofs during winter and snow-covered periods in cold climate regions. The present study attempted to address this gap by validating the use of a snow module in simulating the dynamics of snow accumulation and melting of green and grey roofs. Then, the validated model was used to identify and separate the different events that occur in winter (melt only, rainfall only, rain-on-snow) to assess the hydrological performance of six different configurations of green and grey roofs in Trondheim, Norway. The snow module accurately simulated snow accumulation and melting of green and grey roofs. The results showed that rain-on-snow events in winter have longer duration compared to other events including rainfall events in summer. Consequently, rain-on-snow events yield a higher amount of inflow to the roofs compared to rainfall events in summer, despite summer events having higher intensities. The retention and detention performances of green

**Abbreviations:** *Cfr*, Refreezing factor [–]; *CPRO*, Water holding capacity of snow [–]; *Cx*, Melting factor [–]; *DW*, Drainage water storage [mm]; *INF*, Infiltration value [mm]; *k*, outflow parameter [–]; *Melt*, Actual Melting; *Mr*, Inflow to the roof [l/min]; *n*, Outflow parameter [–]; *Pcorr*, Rain correction factor [–]; *PM*, Potential melting; *Pr*, Peak outflow reduction [%]; *PR*, Potential refreezing; *Q*, Outflow from roof [l/min]; *Q<sub>BR</sub>*, Outflow from Black roof [l/min]; *Q<sub>GR</sub>*, Outflow from Green roof [l/min]; *Rain*, Actual melting; *Refreeze*, Actual refreezing; *Rr*, Event retention ratio [–]; *Scorr*, Snow correction factor [–]; *SN*, Solid snow storage [mm]; *S*, Temporarily stored melted water; *SW*, Liquid snow storage [mm]; *Ta*, Air temperature [C]; *Tc*, Threshold temperature for snow/rain [C]; *Tx*, Threshold temperature for melting/refreezing [C].

\* Corresponding author.

E-mail address: [noelie.maurin@sintef.no](mailto:noelie.maurin@sintef.no) (N. Maurin).

<https://doi.org/10.1016/j.scitotenv.2024.174132>

Received 14 March 2024; Received in revised form 22 May 2024; Accepted 17 June 2024

Available online 20 June 2024

0048-9697/© 2024 The Authors. Published by Elsevier B.V. This is an open access article under the CC BY license (<http://creativecommons.org/licenses/by/4.0/>).

and grey roofs were found to be lowest for rain-on-snow events compared to other types of events, but still yielding significantly lower peak runoffs when compared to standard black roofs. The decrease in retention and detention performances in winter were attributed to the long duration of events, accumulation effect of snow, freezing of roof surface layers, and reduction of evapotranspiration. The study highlights the importance of considering winter conditions in the design of green and grey roofs in cold climates to enhance stormwater management.

## 1. Introduction

Green infrastructures (GI) have emerged as promising and sustainable measures for effectively managing stormwater in urban catchments, thereby addressing the negative consequences of climate change and rapid urbanization (Shafique et al., 2018). GI measures include infiltration swales (Bosco et al., 2023), bioretention cells, green roofs (Stovin, 2010), and grey roofs (Hamouz et al., 2018). Green and grey roofs aim to reduce the amount and attenuate the peaks of stormwater runoff (Johannessen et al., 2018; Krasnogorskaya et al., 2019; Zhang et al., 2021) while providing ecological and environmental benefits such as reducing the urban heat island effects (Susca et al., 2011) and energy consumption of buildings (Bevilacqua, 2021). Moreover, green and grey roofs contribute to enhancing biodiversity within urban catchments (Wooster et al., 2022) while providing aesthetic and recreational values to their surroundings (Jungels et al., 2013).

In the context of stormwater management, green and grey roofs are evaluated based on their retention and detention performances. The former refers to the permanent reduction of stormwater volume through evapotranspiration (Stovin et al., 2013). On the other hand, detention is the delay and attenuation of stormwater outflows, as a result of routing water within the layers of the green roof (Stovin et al., 2017).

Numerous studies have quantified the detention and retention of green and grey roofs in various climatic regions (Hamouz and Muthanna, 2019; Johannessen et al., 2018; Palla et al., 2011; Santos et al., 2023; Sims et al., 2016; Stovin et al., 2012; Yin et al., 2019). For instance, in a Mediterranean climate, Santos et al. (2023) analyzed data from artificial rainfall events on a green roof in Lisbon, reporting retention values between 37 % and 100 % per event and peak attenuation ranging from 30 % to 100 %. In a subtropical climate, Yin et al. (2019) assessed the hydrological performance of a green roof in Nanjing, China, observing high retention (mean per-event retention of 60 % and 30 % accumulated retention) and peak reductions up to 96 %. They also noted a decrease in green roof performance with increased rainfall intensity and amount. In wet and cold climates, green roofs were found to achieve high retention performance, ranging from 11 % to 59 % annually (Bengtsson et al., 2005; Johannessen et al., 2018; Stovin et al., 2013). In addition, green roofs were found to achieve high peak attenuation (ranging from 59 % to 90 %) demonstrating high detention performance (Johannessen et al., 2018; Stovin et al., 2012).

Despite these findings, most literature on green and grey roof performance excludes winter and snow-covered periods in cold climates. A limited number of studies have attempted to quantify the hydrological performance of green and grey roofs under such conditions (Braskerud and Paus, 2022; Hamouz et al., 2018). Hamouz et al. (2018) analyzed the hydrological performance of a grey roof during winter and summer months, reporting a low retention of only 2 % during the winter period. However, detention of the roof was not calculated during winter due to uncertainties related to calculation of antecedent snow depth of winter precipitation events. Braskerud and Paus (2022) analyzed long-term data (11 years) from three green roofs to evaluate their hydrological performance during winter. They found the green roofs to retain 16 % - 19 % of precipitation during winter compared to a traditional reference roof. Furthermore, the green roofs significantly reduced hourly outflow rates during winter compared to the traditional roof. Interestingly, despite higher rainfall intensities in summer, the maximum hourly outflow rates of the green roofs were higher during winter conditions, as

a result of the combined effect of rain and snow melt (Braskerud and Paus, 2022).

The existing research on evaluating the performance of green roofs during winter and snow-covered periods is limited, highlighting the need for further studies in this area. This is particularly important for effective stormwater management in cold climate regions, which represents 24 % of the global land, consisting of thirteen out of the largest one thousand cities globally (Kratky et al., 2017). In cold climate regions, rain-on-snow events that occur during winter have been identified as a significant cause of flooding and its associated negative consequences for urban catchments (Li et al., 2019; Sezen et al., 2020). (Andradóttir et al., 2021) found rain-on-snow events to cause more flooding and damages in winter, compared to summer events in an urban catchment in Iceland.

Improved understanding of the winter performance of green infrastructure can lead to the development of accurate hydrological models. These models are crucial in evaluating the hydrological performance of green infrastructure under different climate conditions. This particularly important for cold climate regions as precipitation patterns are expected to change by climate change, especially in Norway where future climatic scenarios suggest that the country will experience increased precipitation and changes in precipitation patterns in winter (Lind et al., 2023; Vormoor et al., 2016).

Hydrological models also play an important role in the implementation of stormwater management strategies. In Norway, for example, the 3 Step Approach (3SA) is used for stormwater management. Under this strategy, low intensity precipitation should be managed locally using retention-based solutions (step 1), medium-intensity precipitation is addressed with detention-based solutions (step 2), and extreme precipitation is safeguarded by a secure floodway (step 3). Hydrological models can be used in quantifying the performance of green infrastructure within steps 1 and 2. Moreover, they can assess the extent to which green infrastructure may fail under extreme conditions in order to design robust floodways and other flood protection measures.

While numerous hydrological models for green and grey roofs have been developed and validated for summer conditions (Abdalla et al., 2022, 2021; Palla et al., 2012; She and Pang, 2010; Soulis et al., 2017), only one study was found to simulate runoff from a grey roof in winter and snow-covered in cold climates (Hamouz and Muthanna, 2019). They applied the Storm Water Management Model (SWMM) to simulate runoff from a grey roof under both summer and winter conditions. However, poor simulation results during winter were reported due to challenges associated with snow-melt modelling.

The present study attempted to improve understanding and modeling of the hydrological performance of green and grey roofs during winter months in cold climate regions, which could be generalized to other green infrastructure measures (e.g., bio-retention cells, permeable pavement, vegetated swales). Our hypothesis is that runoff from the snowpack to the roof, the roof being either black, green or grey, is dependent only on air temperature and the state of the snowpack (i.e. fraction of solid, liquid). Thus enable the study of the following specific objectives:

- Evaluating the accuracy of a conceptual hydrological model in simulating snow accumulation and melting of green and grey roofs during winter in a cold climate region.

- Developing a method to categorized winter events into different types of events (rain, rain-on-snow, melt)
- Investigating the hydrological performance of different green and grey roof configurations during winter events (rain, rain-on-snow, melt) and summer events in comparison to a standard black roof.

2. Materials and methods

2.1. Høvringen test site

The study was conducted using data collected from a site in Høvringen, Trondheim, Norway. Trondheim is classified in the interface between oceanic (Cfb) and subarctic (Dfc) climates zones according to the Köppen-Geiger climate classification and experiences short summers and cold winters (Hamouz et al., 2018). The Høvringen site has three full-scale roofs, each with a total area of 100 m<sup>2</sup> and a longitudinal slope of 2 %. Two of these roofs were used to test over three generations (2017–2018, 2018–2021 and 2021–2023), six different configurations (i.e., top layer, substrate and drainage) of green and grey roofs, as detailed in Table A1 in the Supplementary Materials. The third roof was kept as a regular black roof for comparison.

Meteorological data (precipitation, air temperature, wind speed and direction, air humidity) were collected with a minute time step from Høvringen site. For each roof, outflow and substrate/surface temperature were collected separately with a minute time step. Precipitation was measured by a heated tipping bucket rain gauge (Lambrecht meteo GmbH 1518 H3) with an accuracy of 2 % while the outflow was measured using an automated weighting bucket, with an accuracy class of C3 according to OIML Certification System. Air temperature was

registered using a thermosensor (Vaisala HMP155A), wind speed using an ultrasonic anemometer (Lufft VENTUS Ultrasonic anemometer) and roof temperature was registered using a temperature sensor Campbell Scientific with uncertainty 0.03C. Additionally, pictures of each of the three roofs were taken every hour. More detailed descriptions of Høvringen site, data collection and processing, and the characteristics of the roofs can be found in Hamouz and Muthanna (2019) and Hamouz et al. (2018).

2.2. The hydrological models

The hydrological models used in this study are the snow routine of the Hydrologiska Byrans avdelning for Vattenbalans (HBV) model for simulating snow melting and accumulation, and reservoir routing models for simulating runoff from the roofs, as shown in Fig. 1. The HBV model is a conceptual lumped hydrological model initially developed in the 1970s by the Swedish Meteorological and Hydrological Institute (Bergström and Forsman, 1973). The HBV model is widely used in simulating runoff of large scale catchments (Seibert and Bergström, 2022). Although it has undergone updates and has been widely utilized in various studies, its general structure has remained largely unchanged (Lindström et al., 1997).

The reservoir routing models are commonly used for simulating outflows of green roofs (Abdalla et al., 2022; Palla et al., 2012; Soulis et al., 2017; Vesuviano et al., 2013). Albeit their simplicity, the reservoir model were shown to simulate water outflow with a high level of accuracy that is comparable with physically-based models (Palla et al., 2012; Soulis et al., 2017). Nevertheless, the reservoir models were not evaluated before in simulating runoff during snow periods.

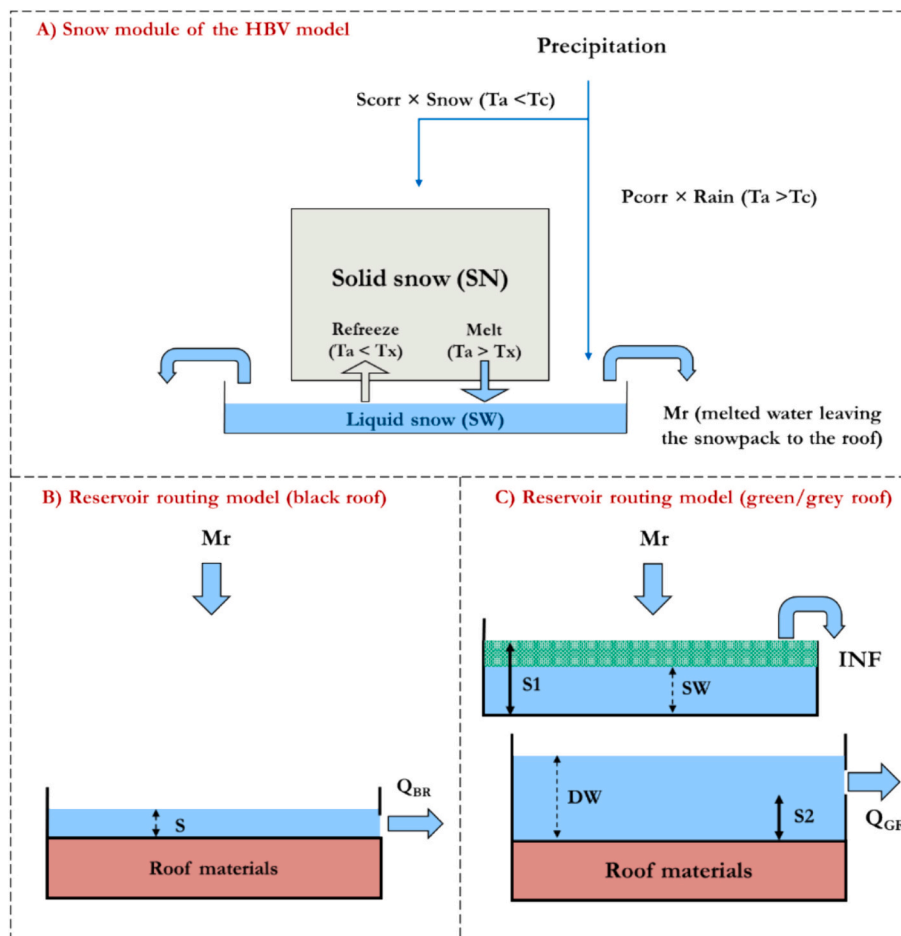


Fig. 1. Models used in the study.

The coupling of these two models (i.e., the reservoir model and the HBV snow module) has not been tested before for green roofs and stormwater purposes. The rationale for selecting the HBV model in this study is that it requires only readily available air temperature and precipitation data to simulate snow accumulation and melting, making it beneficial for practical applications.

2.2.1. Snow routine of the HBV model

The snow routine of HBV uses air temperature ( $T_a$ ) to separate snow and rain, based on a threshold value ( $T_c$ ). Both Rain (Rain) and Snow (Snow) time series are multiplied by correction factors (Pcorr and Scorr) to account for measurement errors (Eqs. (1)–(2)). The snow increases the solid snowpack (SN) while the rain is stored in the liquid snow storage (SW), as shown in Fig. 1. If the air temperature exceeds a threshold value ( $T_x$ ), the solid snow starts to melt, while if the temperature dropped below the same threshold value ( $T_x$ ), the liquid snow storage freezes. Each time step, the model determines a potential melting (PM) and a potential refreezing (PR) value based on the air temperature, using Eqs. (3)–(4). These potential values are used to determine the actual melt (Melt) and refreezing (Refreeze), based on the available solid and liquid snow using Eqs. (5)–(6).

$$Snow = Snow \times Scorr \tag{1}$$

$$4Rain = Rain \times Pcorr \tag{2}$$

$$PM_t = \max(Cx \times (T_a - T_x), 0) \tag{3}$$

$$PR_t = \max(Cfr \times Cx \times (T_x - T_a), 0) \tag{4}$$

$$Melt_t = \min(PM_t, SN_t) \tag{5}$$

$$Refreeze_t = \min(PR_t, SW_t) \tag{6}$$

$$Mr_t = \max(SW_t - (CPRO \times SN_t), 0) \tag{7}$$

$$SN_{t+1} = SN_t - Melt_t + Snow_t + Refreeze_t \tag{8}$$

$$SW_{t+1} = \min(SW_t + Melt_t + Rain_t - Refreeze_t, CPRO \times SN_t) \tag{9}$$

Here  $Cx$  and  $Cfr$  are melting factor and refreezing factor respectively of the snowpack.  $CPRO$  represents the water holding capacity of snow.

If  $SW$  exceeds the water holding capacity of the snowpack ( $CPRO \times SN$ ), the melted water ( $Mr$ ) leaves the snowpack to the roof surface below (Eq. (7)). After each time step, both the liquid and solid storage are balanced using Eqs. (8) and (9).

2.2.2. The reservoir models

Melted water from the snowpack ( $Mr$ ) is employed in the reservoir models to simulate runoff. For the black roof,  $Mr$  is temporarily stored ( $S$ ) and used to calculate the outflow of the roof ( $Q_b$ ) using Eq. (10), which uses an empirical power equation with two parameters ( $k$  and  $n$ ). For green and grey roofs, the reservoir model consists of two tanks representing the substrate and drainage layers of the roofs.  $Mr$  enters the substrate layer, saturating its storage capacity ( $S1$ ). When the substrate layer's storage limit is exceeded, water infiltrates (INF) into the lower tank, following Eq. (12). Simultaneously, the drainage layer stores water ( $S2$ ), and water discharge ( $Q_{GR}$ ) starts once the drainage layer reaches its storage capacity, as described by Eq. (13).

It's worth noting that the reservoir model for green and grey roofs does not account for the evapotranspiration (ET) process. The Oudin formula for ET (Oudin et al., 2005), typically most appropriate for cold climate regions (Almorox et al., 2015), assigns an ET value of zero when the average daily temperature drops below 5 degrees Celsius, which is often the case during winter in cold climate regions. Hence ET was ignored in the model in this study.

$$Q_b = k \times Stn \tag{10}$$

$$S_{t+1} = \max(S_t + Mr_t - Q_t, 0) \tag{11}$$

$$INF_t = k1 \times (\max(SW_t - S1, 0))^n \tag{12}$$

$$Q_{GR} = k2 \times (\max(DW_t - S2, 0))^n \tag{13}$$

$$SW_t = (SW_{t-1} + Mr_t - S1, 0) \tag{14}$$

$$DW_t = (DW_{t-1} + INF_t - S2, 0) \tag{15}$$

Here,  $INF_t$  is the infiltration value at time  $t$  which represents the inflow from the substrate layer to drainage layer and  $DW$  stands for drainage water storage.

2.3. Calibration and validation of the model

The hydrological model consisting of the two modules (i.e., snow module and reservoir routing) was used to simulate the snow accumulation and melting of the black roof. The model has seven parameters that need to be estimated by calibration (five for the snow module and two for the reservoir routing). For the green and grey roofs, the HBV snow module parameters were fixed from the calibration of the black roof while the parameters of the reservoir model (6 parameters) were calibrated for each of the three generations of green/grey roofs. Selected calibrated and validation periods of the green and grey roofs are presented in Table 1.

In order to calibrate the models, the differential evolution algorithm (DE), was implemented through the Deoptim library in R (Mullen et al., 2011). This algorithm generates populations of candidate solutions to an optimization problem. Each new population is derived from the previous one, with the objective of improving or maintaining the same objective function value for each candidate in the next generation. The calibration process involved 100 generations, with a number of 200 candidates in each population. The best candidate in the last population (based on objective function value) was considered the optimal.

The DE algorithm searches for the optimal values of each parameter within a user-defined range, as presented in Table A3 in the Supplementary materials. These limits were selected based on relevant studies in the literature (Abdalla et al., 2022; Chen et al., 2017). The calibration and validation of the snow module and the black roof was conducted using a winter period from November 2017 to April 2018, while two separate winter periods, 2018–2019 and 2020–2021, were utilized for validation. For green and grey roof, different periods were selected for calibration and validation of the different generations, as summarized in

**Table 1**  
Calibration and validation results of the green and grey roofs.

Roof	Generation	Simulation periods		Simulation accuracy (KGE)	
		Calibration	Validation	Calibration	validation
Roof1	Generation1	2017/11/01–2018/04/29	2017/02/20–2017-04-29	0.8439	0.7606
	Generation2	2018/11/15–2019/04/29	2020/11/01–2021/04/29	0.7688	0.8292
	Generation3	2022/11/01–2023/04/10	2021/11/01–2022/01/15	0.8455	0.8855
Roof3	Generation1	2017/11/01–2018/04/29	2017/02/20–2017-04-29	0.8993	0.6396
	Generation2	2018/11/15–2019/04/29	2020/11/01–2021/04/29	0.7873	0.7111
	Generation3	2022/11/01–2023/04/10	2021/11/01–2022/01/15	0.8806	0.9237

**Table 1.** All simulations were performed with a one-minute time step.

The Kling-Gupta Efficiency (KGE) (Gupta et al., 2009) between the simulated and observed runoff of the roof was chosen as the objective function for both calibration and validation. KGE combines three statistical metrics to evaluate hydrological model performance (equation): correlation, residual error, and volumetric error, using the following formula:

$$KGE = 1 - \sqrt{(r - 1)^2 + (\alpha - 1)^2 + (\beta - 1)^2} \quad (16)$$

$r$  is the correlation coefficient between simulated and observed outflow,  $\alpha$  is the residual error (measure of flow variability error) and  $\beta$  is the volumetric error (bias). According to (Thiemig et al., 2013), values of KGE can be used to classify model results as follows:

- Good ( $KGE \geq 0.75$ )
- Satisfactory ( $0.75 > KGE \geq 0.5$ )
- Poor ( $0.5 > KGE$ )

In addition, the model was validated using Nash Sutcliffe Efficiency (NSE) (Nash and Sutcliffe, 1970).

#### 2.4. Characterization of winter events

The calibrated snow module of the HBV model was used to identify and characterize the various types of events that occur during winter and snow-covered periods. In this study, a **snow-covered period** is defined by the presence of snow on the roof, starting when snow begins to accumulate and continuing until the entire snowpack upon the roof has melted away. This period can last for weeks and involves multiple events of snow accumulation and melting, which impact the outflow from the roofs. Further, a **winter event** is an event that results in an inflow to the roof surface during winter periods (defined by the presence of snow), either due to rainfall, snow melting or a combination of both, called rain-on-snow event. Studying the dynamics of these accumulation and melting events is important to better quantify the hydrological performance of green and grey roofs during winter conditions.

In the literature of green infrastructure, continuous time series are typically divided into separate rainfall events to determine event-based indicators such as peak reduction, per-event retention, centroid and peak delay, etc. A period of 6 h of dry (i.e. sum of rainfall = 0) is often used to separate consecutive rainfall events (Stovin et al., 2017; Johannessen et al., 2018). However, this criterion proves inadequate during winter, as snow events can persist on roof surfaces (both black and green/grey roofs) for prolonged duration. This makes it challenging to adequately compare the hydrological performance of green roofs with the standard black roof.

In this study, we developed a methodology using temperature and time for separating precipitation time series in winter into separate events. The methodology relies on the time series data of  $Mr$  as derived from the calibrated HBV model, along with the time series of rainfall (the precipitation occurring when  $T_a > T_c$ ). Winter events were separated based on a period of 6 h, during which the total inflow to the roof  $Mr$  equals zero. We identified three different event types in winter: Snow melt only, rain only, and a combination of both (rain-on-snow). These can be characterized as follows:

- Rain event: the sum of  $Mr$  equals the sum of rainfall.
- Melt event: the sum of  $Mr$  is  $>0$ , while the sum of rainfall is 0.
- Rain-on-snow event (Rain + Snow melt): the sum of  $Mr >$  the sum of rainfall  $>0$ .

In this study, the periods were selected as 6 h for separating winter events to allow for comparison with summer events. Winter and summer events with an amount  $<2$  mm were omitted from the analysis to exclude minor, insignificant events.

#### 2.5. Selected performance indicators of green roofs

The hydrological performance of the green and grey roofs was assessed in winter months and compared with summer months. Winter and summer months were defined by the existence of snow melt events and rain-on-snow events. Peak outflow reduction ( $Pr$ ) and event retention ( $Rr$ ) were determined for each event, using Eqs. (10) and (11), to compare the performances of the green roofs with respect to the simulated black roof performance.

$$Pr = 100 \times \frac{\max(Q_{BR}) - \max(Q_{GR})}{\max(Q_{BR})} \quad (17)$$

$$Rr = \frac{\sum \text{Inflow} - \sum Q_{GR}}{\sum \text{Inflow}} \quad (18)$$

where  $Q_{BR}$  and  $Q_{GR}$  are black and green roof / grey roofs outflow, respectively.

#### 2.6. Trends in winter and summer events from long term simulation

Using the calibrated hydrological model, a long-term simulation (1989–2020) was conducted using precipitation and temperature data of meteorological station in Trondheim. The number and characteristics of winter and summer events were determined. To assess whether a significant trend exists in the frequency of these events, the Sieve-bootstrap Student's  $t$ -test was employed (Hall and Keilegom, 2003).

### 3. Results and discussion

#### 3.1. Calibration and validation of the hydrological models

The DE algorithm was used to calibrate the hydrological model, using measured outflow from the roof. The optimal parameters found by the algorithm are presented in Table A3 in the Supplementary materials. Fig. 2 shows the simulated and observed hydrographs of the black roof, and Figs. A2–A5 in the Supplementary materials show the simulated and observed runoff of the green and grey roofs for calibration and validation periods. As noted, the calibrated model yielded simulations with KGE of 0.87 for the calibration period, which is considered good modelling results. In addition, the model yielded good performance in both validation years ( $KGE > 0.75$ ). For green and grey roofs, the coupled snow and reservoir models yielded good calibration results, with KGE values ranged between 0.77 and 0.89 for the three generations, and satisfactory to good validation results, with KGE ranging between 0.64 and 0.92, as summarized in Table A2.

The DE algorithm produced values of 1.04 and 1.31 for  $pcorr$  and  $scorr$ , respectively. As previously discussed, these parameters compensate for measurement inaccuracies in precipitation gauges. The calibration outcomes suggest that errors in snowfall measurement are larger than those for rainfall, reaching up to 30 %. This aligns with existing literature, where it has been shown that measurement errors for snow by precipitation gauges can reach up to 50 % due to wind effects (Yang et al., 1999). In the absence of corrections for precipitation measurements (i.e., setting  $pcorr$  and  $scorr$  to 1), the calibration and validation for the hydrological models were found to be less accurate. Fig. A1 in the Supplementary materials demonstrates the calibration and validation outcomes for the black roof without the calibration of  $pcorr$  and  $scorr$  parameters, showing reduced simulation accuracy. Moreover, Fig. A1 illustrates that the cumulative volume on the black roof exceeds the volume of measured precipitation, due to the underestimation of measured snow by the precipitation gauge.

The DE algorithm produced low values for the storage parameters ( $S1$  and  $S2$ ) for the green and grey roofs, as illustrated in Table A3. These values are significantly lower than the retention storage capacities of the roof layers, which, according to existing research on green roofs, range

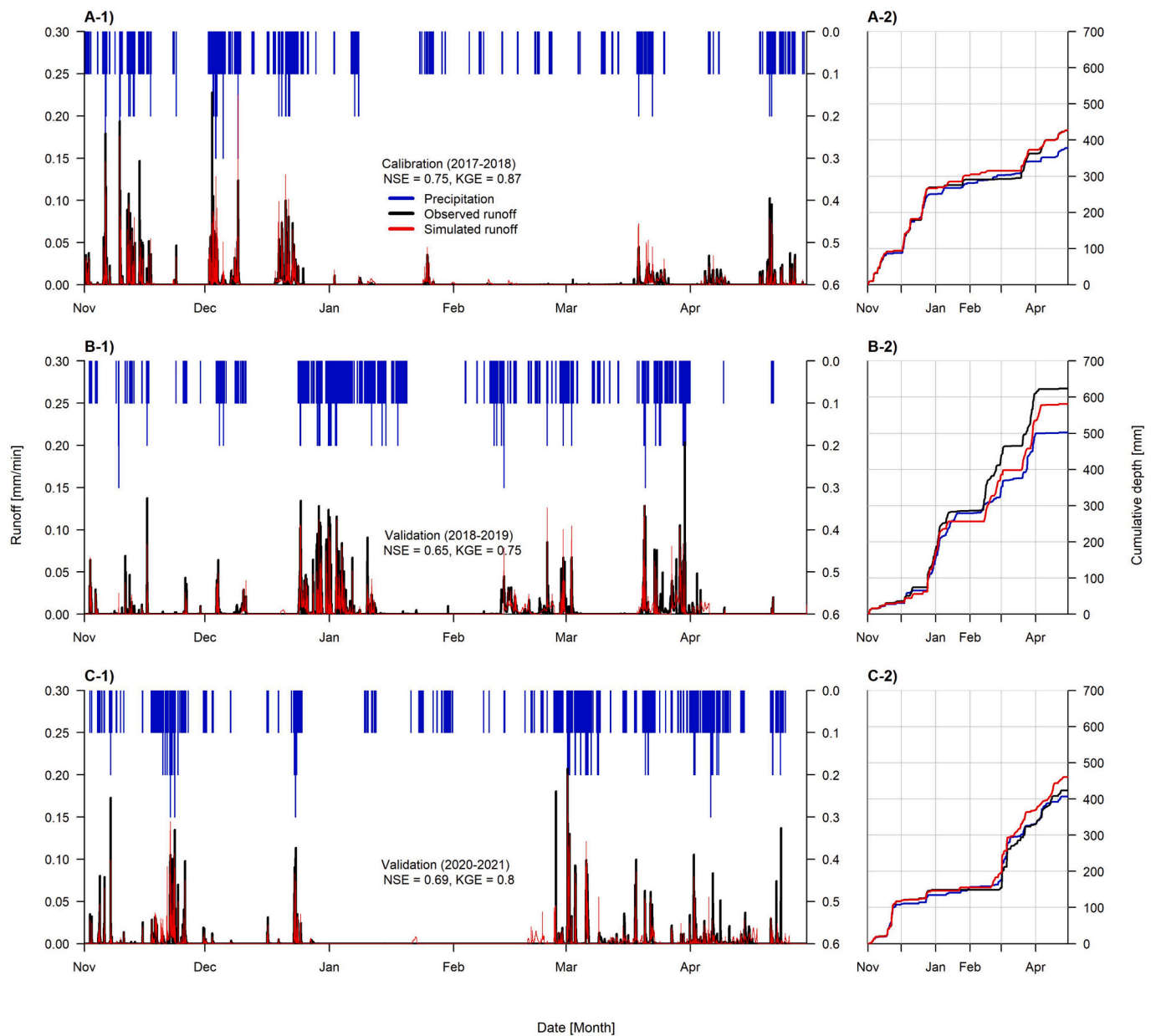


**Fig. 2.** Calibration and validation results of the hydrological model. A-1 compares the simulated and observed runoff during the calibration period. B-1 and C-1 show the comparison between simulated and observed runoff for the first and second validation periods, respectively. A-2, B-2, and C-2 illustrate the cumulative depth of precipitation along with observed and simulated runoff for the calibration period and the two validation periods, respectively.

between 20 and 25 % of the substrate thickness (Johannessen et al., 2018; Stovin et al., 2013). Nonetheless, the omission of evapotranspiration (ET) in the models means that these parameters do not reflect the true retention storage of the green and grey roofs. Instead, they represent the initial storage deficits at the start of the simulations.

In this study, the hydrological models exhibited satisfactory performance, leading to the conclusion that the snow module of the HBV model is suitable for simulating winter runoff across various green and grey roof configurations. The study by Hamouz and Muthanna (2019) identified that the SWMM model yielded poor simulation results for winter runoff of a grey roof (Roof1 - generation 1 in this study). The poor performance of the SWMM model was attributed to the unsuitability of its snow module. While both the SWMM and HBV models employ the same equation for calculating snowmelt from air temperature (Eq. (3)), there are differences between the models and the calibration procedures between the two studies that lead to improved simulation accuracy in this study. Firstly, unlike SWMM, the HBV model incorporates

refreezing of melted water which affect model outcomes, particularly regarding the starting and the volume of melting events. Secondly, the SWMM model does not include correction parameters for snowfall and rainfall measurements (pcorr and scorr), leading to an underestimation of runoff from green roofs during winter months, as discussed earlier. It is important to highlight that calibrating snow and rainfall correction parameters is a common practice in catchment modelling for conceptual hydrological models like the HBV model (Seibert, 1997). However, this practice is not followed in the modelling GI measures within the existing literature.

Other factors contributing to the SWMM model’s poor performance during winter are related to the calibration of the model (Hamouz and Muthanna, 2019). The threshold temperatures for rain/snow and melting ( $T_c$  and  $T_x$ ) were not calibrated but fixed to zero. In contrast, the present study found that the optimal values for  $T_c$  and  $T_x$  to be slightly above zero. Additionally, Hamouz and Muthanna (2019) calibrated the grey roof parameters only under summer conditions and

applied them to simulate winter months, while only calibrating the snow module. However, it is expected that some roof parameters would vary between winter and summer in cold climate regions due to physical changes in some of the roof layers. For example, the surface layer of the grey roof freezes intermittently during winter, as shown in Fig. A6 in the Supplementary materials, resulting in decreased infiltration to the substrate layer.

### 3.2. Characterization of a snow-covered period

The calibrated snow module of the HBV model was used to characterize a snow-covered period that occurred between November–December of 2019 which is shown in Fig. 3. Fig. A6 presents photos taken of the three roofs at different times (P1, P2, P3 and P4) during the snow-covered period. The methodology for separating winter events (as described in Section 2.4) was applied to the snow-covered period, resulting in three rain-on-snow events and one melt event as shown in

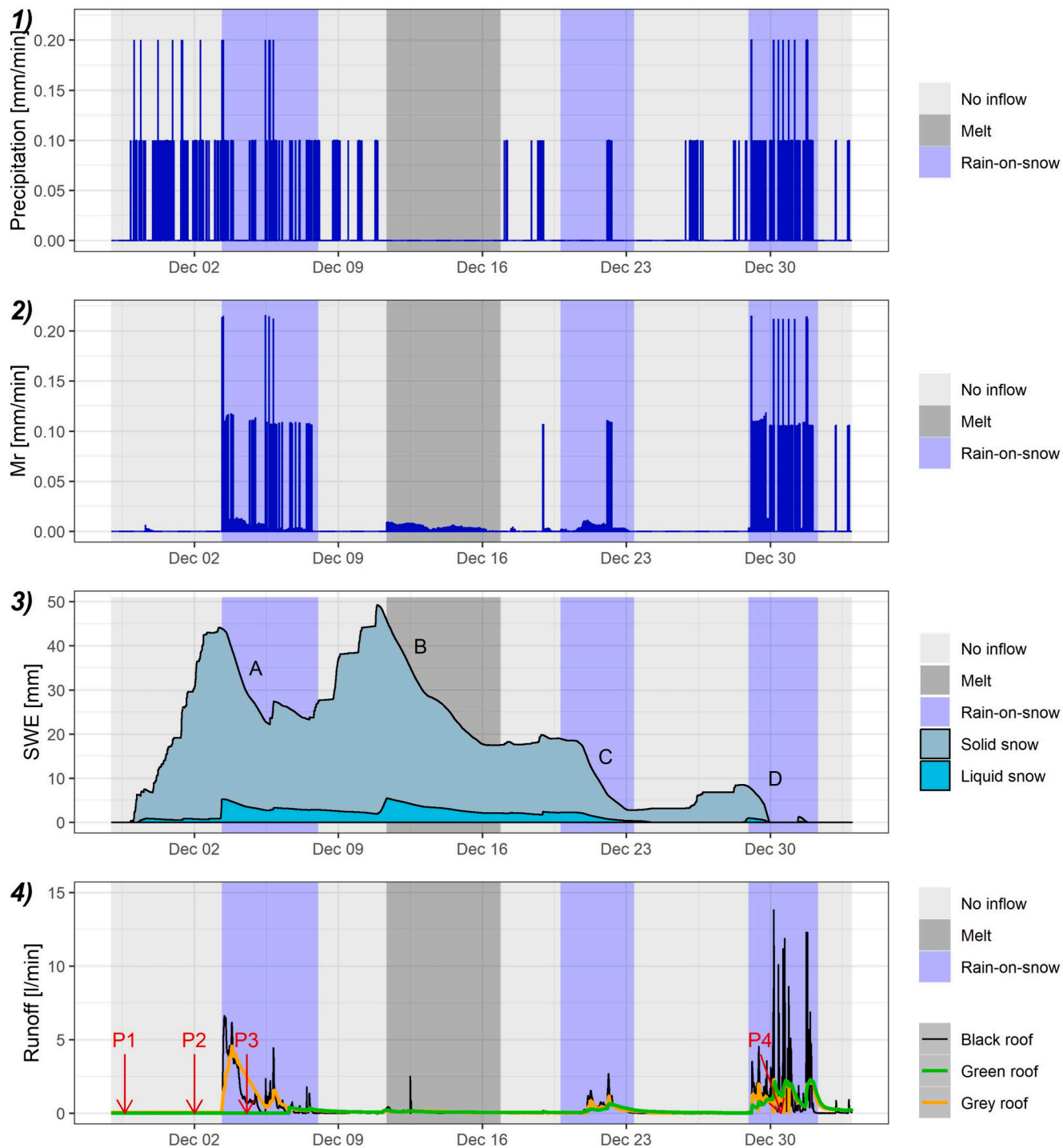


Fig. 3. Measurements and model outputs of a snow-covered period during November–December 2019 at Høvringen, Norway. The graph shows from top to bottom; 1) Precipitation, 2) melted water leaving the snowpack to the roof (Mr), 3) snow water content (SWC), and, 4) roofs outflows. Precipitation and outflow data are measured at the site, whereas the hydrological model provides estimations for snow water content (SWC), and Mr. See text for explanation of A-D and P1-P4.

Fig. 3.

As shown in Fig. A7, it can be noted that the black roof surface temperature was closely following the air temperature, varying from  $-14$  to  $+9$  degrees Celsius. In contrast, grey roof substrate temperature was steady and close to zero, meaning that the roof was frozen during the snow-covered period. Since the extra layer consists of an extruded clay type material with a rather small particles and a high water storage capacity, this observation could be explained by a high mass of frozen water stored into the substrate material of the grey roof, increasing its energy storage capacity. The green roof substrate temperature, however, was fluctuating above zero degree, indicating that it remained unfrozen for most of the period.

The first event in the snow-covered period (labelled as “A” in Fig. 3), was categorized as rain-on-snow event. During event A, the black roof exhibited the highest and quickest outflow peaks. Similarly, the grey

roof experienced quick and high outflow, albeit with a slightly lower peak compared to the black roof. This can be attributed to the presence of a frozen layer (visible in image P3 of Fig. A6) preventing water from infiltrating between the pavement stones. In contrast, the green roof surface and its vegetation were not frozen. Consequently, no outflow was observed during event A, indicating that the green roof can be an effective solution to detain melted and rainfall water during a combined event. Only a small volume of water was observed to be released after a delay of a few days. Event C follow the same pattern but at minor scale due to less snow and rain at initial conditions.

The second event, B (Fig. 3), was categorized as a melt event. This event generated the lowest outflow peaks from the roof, although the melted snow depth was larger than other melting events. This highlights the significant role of rainfall in enhancing peak runoff in winter events. This confirms the finding of [Braskerud and Paus \(2022\)](#) in which rainfall

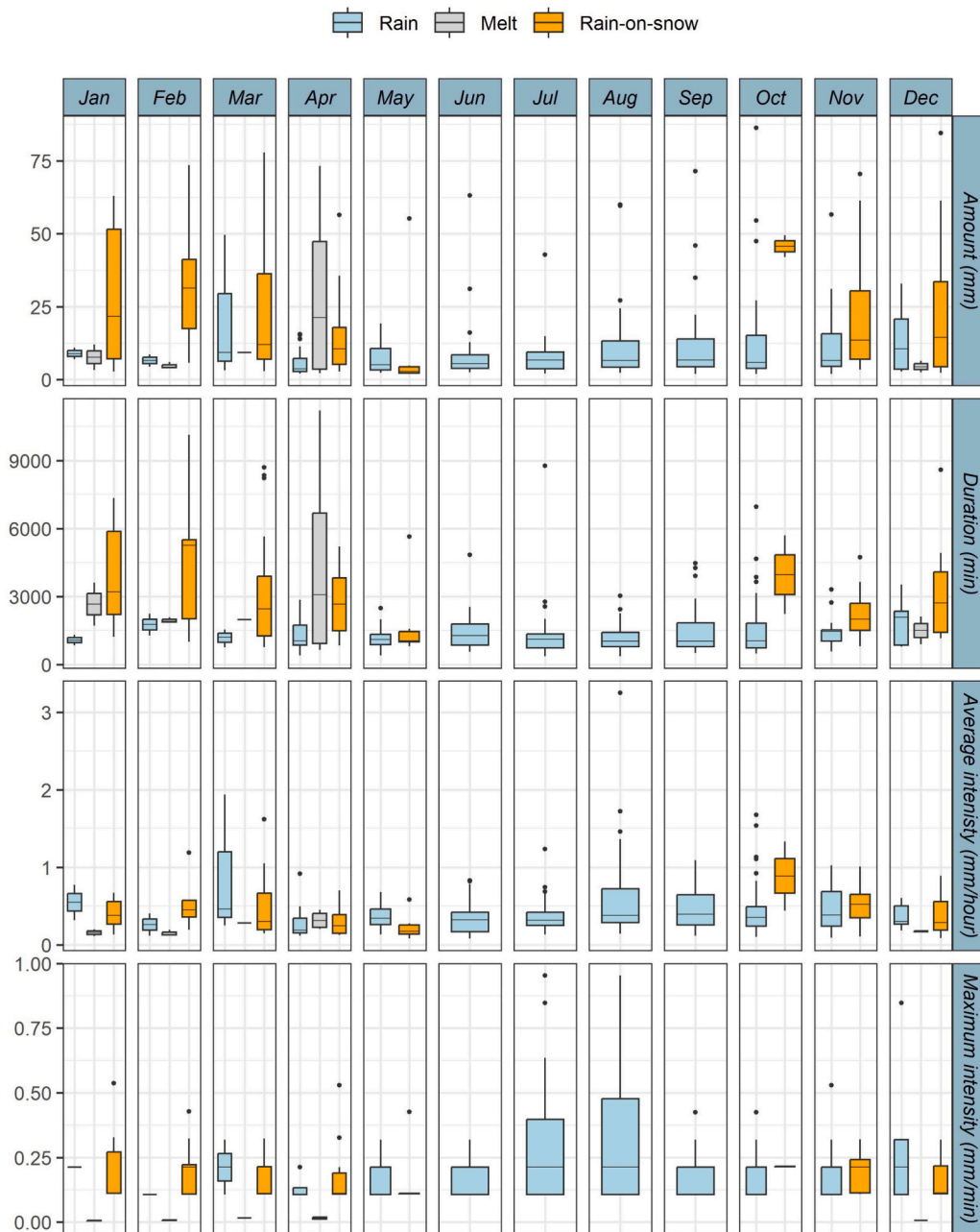


Fig. 4. Properties of snow melt/rain/rain-on-snow events (i.e., amount, duration, and intensity) and properties of rainfall events per month at Høvringen, Norway (2017–2023).



and air temperature were found to be the most influential variables in generating high peaks outflow during snow-covered periods.

Event C and D were both rain-on-snow events. It can be noted that the melted snow depth in event C is larger than in event D, while rainfall amount and intensity were higher during event D. Consequently, runoff values during event D were larger than event C, which suggest that for rain-on-snow events, the intensity and amount of rain are more influential than the melted snow depths in generating high runoff peaks. Runoff values for the black roofs were higher than for the grey and green roofs, which further emphasize that green and grey roof still have better performances than regular black roof in winter conditions. It is believed that both green and grey roof capacities were near saturation prior to event D, due to the reduced evapotranspiration in winter (Hamouz and Muthanna, 2019) and the antecedent melting events. Therefore, it can be noted that the outflow peaks of the green and grey roofs were comparable in this event. However, the grey roof produced slightly faster runoff values than the green roof (which could be attributed to partly frozen surface of the grey roof as seen in image P4 in Fig. A6).

### 3.3. The hydrological performance of green and grey roofs during winter

Fig. 4 shows statistics of the amount, duration, average intensity and maximum intensity of the events registered at Høvringen in the time

span 2017–2023. The summary table of melt, rain and rain-on-snow events characteristics can be found in Table A2 in the Supplementary materials. The events are categorized into rain, melt, and rain-on-snow, as described in Section 2.4. It can be noted from Fig. 4 that the months from June to September only registered rain events. Hence, they were categorized as summer months in this study. On the other hand, the months of May, October and November have experienced rain-on-snow and rain events, while the remaining months have registered all types of events. Following this, the winter months at Høvringen, Trondheim, were defined to be from October to May while the summer months were June to September. It is clear from Fig. 4 that rain-on-snow events have longer duration when compared to other types of events. Consequently, rain-on-snow results in higher amount of inflow to the roofs, even when compared to summer events, despite the latter having higher maximum and average rain intensities.

The retention and detention indicators for summer and winter events were determined for each green and grey roof configuration. Fig. 5 shows box plots for the retention and peak reduction for the different green and grey roofs configurations tested at Høvringen. The box plots show that the retentions for rain events during summer months were slightly higher when compared with the retention of rain events during winter months, whereas melt events have higher retention and less variability. Event retention during summer with value above 50 % for

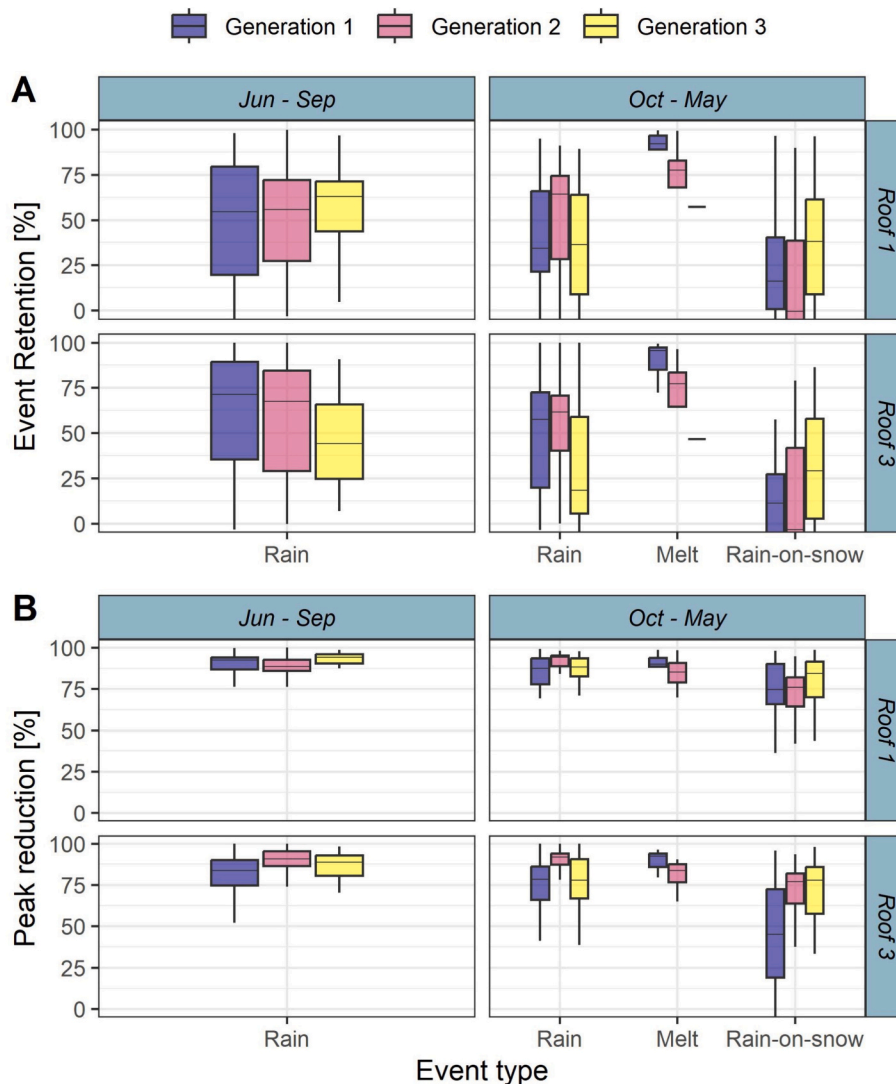


Fig. 5. The hydrological performance of the different configurations of green and grey roofs during winter and summer months. The hydrological performance is measured by two event-based indicators: A) retention [%] and B) peak reduction [%].

roof 1 correspond to the upper limit of event retention percentage found by (Bengtsson et al., 2005; Johannessen et al., 2018; Stovin et al., 2013). On the other hand, rain-on-snow events have the lowest event retention of all types of events.

For roofs detention, the peak reduction rates were higher during the summer months with values above 80–90 %, similarly to the literature (Johannessen et al., 2018; Palla et al., 2011). The minor variations observed between the generations can be attributed to differences in

thickness and water storage capacity of different roofs, as detailed in Table 1. Furthermore, the peak runoff reduction rates during the winter months were found to be comparable to those of the summer months for rain events and melt events but were significantly lower for rain-on-snow events. In particular, the configuration on roof 3 generation 1, characterized by a thin detention layer below a sedum mat, exhibited the lowest peak runoff reductions. For rain-on-snow events, the peak flow reduction can be attributed to the low retention capacity of the

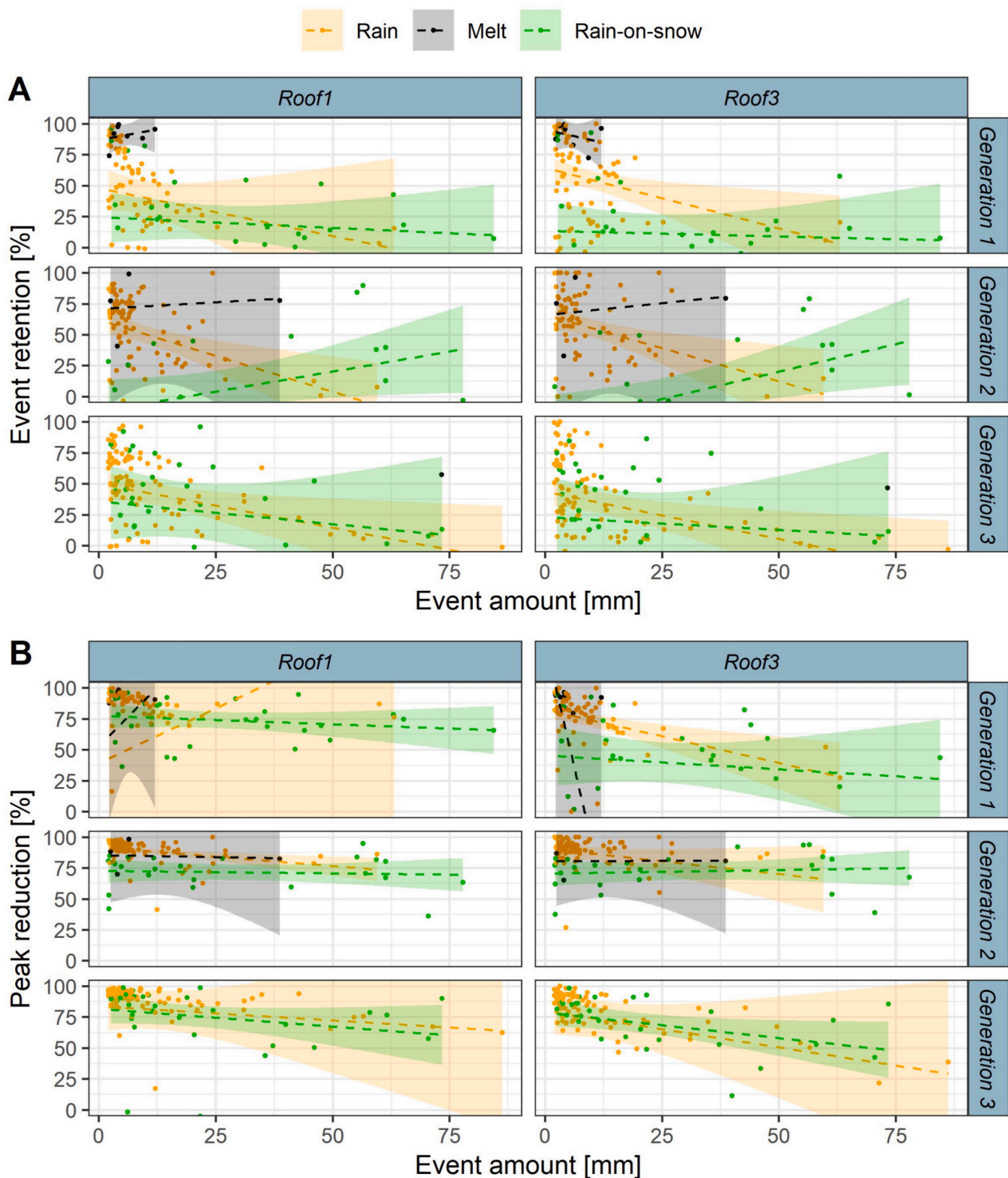


Fig. 6. Comparison of the hydrological performance of the different configurations of green and grey roofs for the different types of events (rain, melt, rain-on-snow) against the amount of rainfall/melt during the event.

roofs. Additionally, as shown in Fig. A6, the partial freezing of the roof's surface layer during snow periods reduces the roof's infiltration capacity, thereby increasing runoff.

Fig. 6 compare the hydrological performances of the different roof configuration, under the same amount, for different types of events (rain, melt, rain-on-snow). As shown in Fig. 6, the retention and detention of the roofs were generally higher during rain events compared to rain-on-snow events for green and grey across all generations, especially for events with amounts <35 mm. This can be explained by the partial freezing of roof surfaces (as shown in Fig. A6) and the reduced storage capacity of the roofs during rain-on-snow events. However, for a few extreme events (amount > 35 mm), retention appears to be equal to or slightly higher for rain-on-snow events. This can be attributed to the longer duration of these extreme events compared to rainfall events (as illustrated in Fig. 4). The long duration of rain-on-snow events may lead to the melting of the frozen surface, thereby allowing the green roof to retain a portion of the event.

Fig. 7 shows statistics of the event peak runoff for the different configurations. It was observed that, during the winter months, both

green and grey roofs demonstrated lower peak runoff rates compared to the standard black roof. Moreover, the configurations tested on roof 3 exhibited higher peak runoff rates than those tested on roof 1, a difference that can be attributed to the thickness of the roof layers, where thicker roofs proved to be more effective at reducing peak runoff. The highest peak runoff was recorded for rain-on-snow events, offering an explanation for why Andradóttir et al. (2021) reported that rain-on-snow events tend to cause more flooding and damage compared to events occurring in the summer.

Figs. 5 and 7 show a large variation for hydrological indicators such as retention, peak reduction and maximum runoff rate for rain-on-snow events. To investigate this, the peak runoff of rain-on-snow events were plotted as function of rain amount for the different roof configurations, as shown in Fig. 8. It is clear that peak runoff of the roofs increases as the amount of rainfall in the rain-on-snow events increases. Indeed, snow acts as a water storage on the roof over long period, and when being triggered by rain, can release the stored water content, and the more rainfall, the fastest the process will be. It can be noted that the peak runoff is lower for roofs with thicker configurations compared to thinner

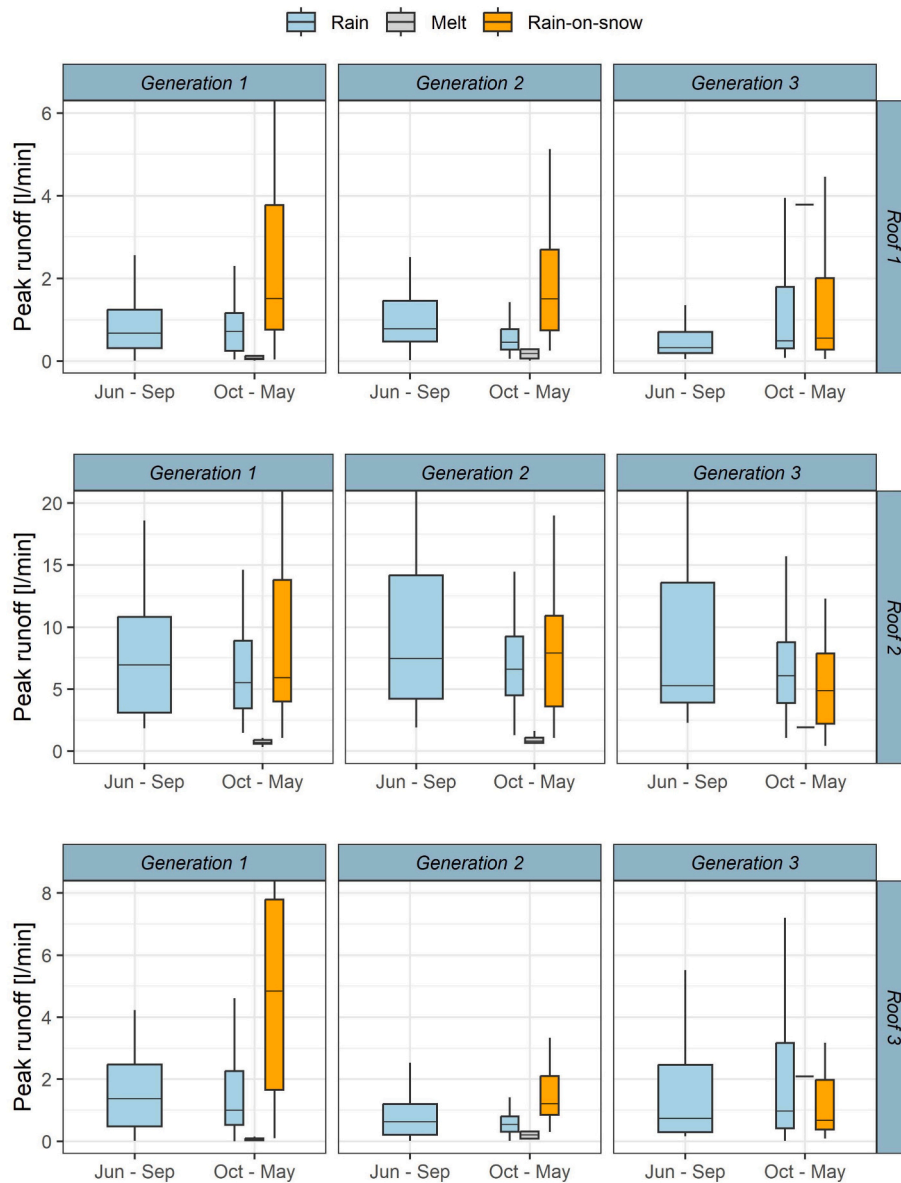


Fig. 7. The hydrological performance of the different configurations of green and grey roofs during winter and summer months compared with the black roofs (roof 2). The hydrological performance indicator is event peak runoff [l/min]. NB the axis scales.

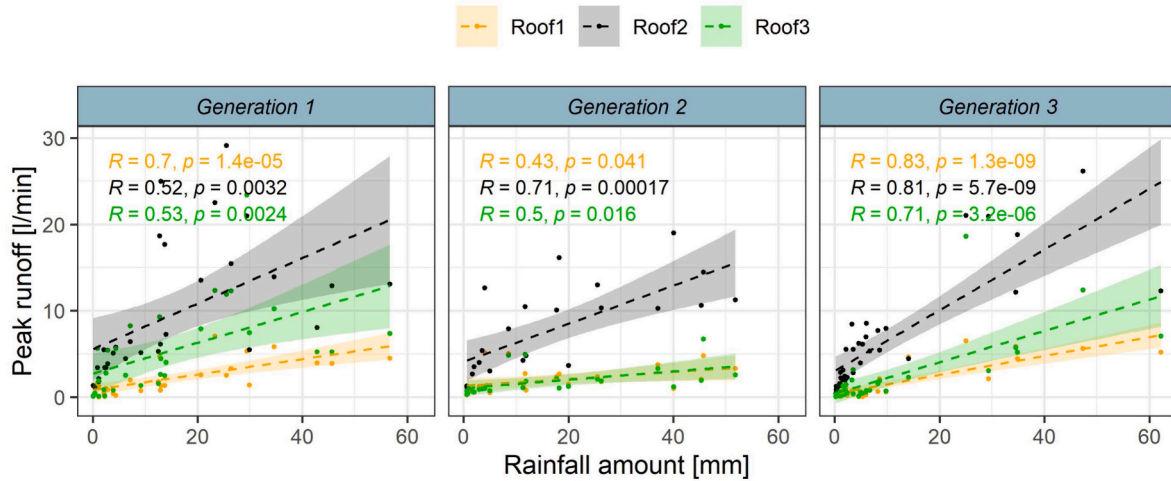


Fig. 8. Correlations between peak runoff and rainfall amounts in rain-on-snow events.

configurations.

### 3.4. Implication for stormwater management in cold climate

The findings from this study indicate that green and grey roofs exhibit worst hydrological performances during rain-on-snow events compared to rain events and melt events. Notably, rain-on-snow events are characterized by longer duration and higher amounts, leading to high runoff peaks from the roofs. When compared with summer events, rain-on-snow events yield higher runoff peaks, despite summer events having higher intensities. However, the current design practices for green roofs and other GI measures in cold climates typically focus only on rain events and summer periods (Pons et al., 2022). This approach may not adequately represent the worst-case scenarios for evaluating the effectiveness of GI measures. Hence, it is crucial in cold regions to

evaluate the performance of GI measures on rain-on-snow events.

The thickness of the green and grey roof was found to influence their hydrological performance, as thicker configurations were found to perform better in winter events, particularly for rain-on-snow events, than thinner configurations. Nevertheless, it should be emphasized that even thinner configurations of green and grey roofs could outperform traditional black roofs in mitigating winter events.

Fig. 9 shows the annual precipitation and the number of events during winter and summer months as function of year in the period 1987–2020. The annual precipitation is divided into snowfall and rainfall for the winter months and the number of events is shown for the three types of winter events. Summer rainfall events showed a minor decreasing trend over the simulated period, both in terms of annual precipitation amount and number of events. On the other hand, the number of events in winter months showed a linear positive trend over

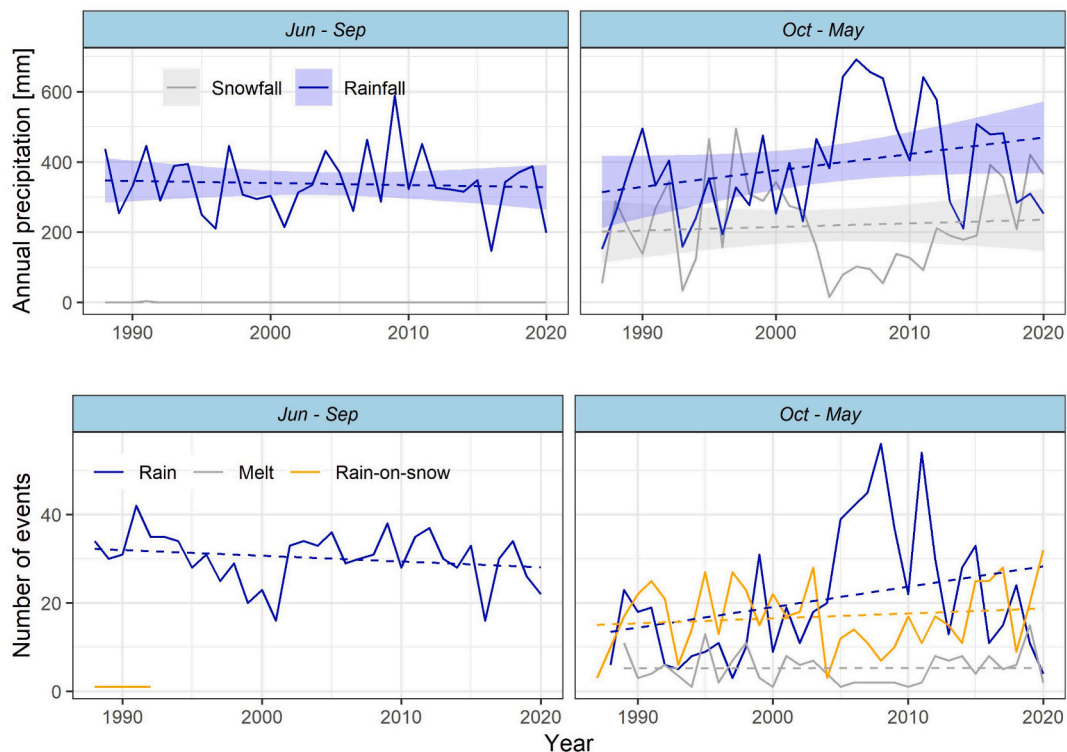


Fig. 9. Number of events and annual precipitation during winter and summer months in Trondheim, Norway in the period 1987–2020.

the years for rain and rain-on-snow events. However, these linear trends were not statistically significant ( $p > 0.05$ ), based on the Sieve-bootstrap Student's  $t$ -test. However, when investigating the trend of number of events for each month, as shown in Fig. A8 in the Supplementary materials, it was found the number of rain events in October showed a positive trend that was statistically significant ( $p < 0.05$ ) based on the Sieve-bootstrap Student's  $t$ -test. This is possibly due to climate change that affects the transitioning between summer and winter periods, and this is likely to continue in the future affecting other months. This was also concluded in a recent study that anticipates climate changes with increasing air temperature will likely change the magnitude and frequency of snow melting and rainfall events in cold (maritime) climates, and hence, increase the number of freeze-thaw cycles (Zaqout et al., 2023). The characteristics of winter and summer events (amount, intensity) were also determined from the long-term simulations (Fig. A9, Supplementary materials). The amounts of rain-on-snow events were consistently higher than other types of events, and even though no significant trend could be observed, this emphasizes the positive benefits of implementing green and grey roofs to better handle stormwater under winter conditions.

#### 4. Conclusion

The present study evaluated the accuracy of a conceptual hydrological model of green and grey roofs coupled with the snow module of the HBV model for snow accumulation and melting during winter months and snow-covered periods in cold climate regions. The coupled conceptual hydrological model and HBV model was found to be well suited to model the runoff during winter events.

Based on the calibrated HBV model the study developed a methodology for separating winter events into three types of events, namely rain events, melt events and rain-on-snow events.

The hydrological performances of six different configurations of green and grey roofs were assessed for the different types of winter events and compared with the performance during summer months. The following list of conclusions was made:

- Rain-on-snow events which contains both accumulated snow and rain, have significantly longer duration compared to other types of events.
- As a result, rain-on-snow events have higher amount of water, resulting in higher peak runoff from the roof, compared to summer events despite the latter having higher precipitation intensities.
- Retention and detention performance of green and grey roofs were found to be lower in winter compared to summer months, especially for rain-on-snow events.
- However, the green and grey roofs were around two times better at lowering peak runoff when compared to standard black roofs during winter events.
- Thicker configurations were found to perform better in winter events, particularly for rain-on-snow events, than thinner configurations.
- The decrease in retention and detention performances in winter is attributed to the long duration and the high inflows of the events, freezing of roof surface layers, and reduction of evapotranspiration.

Overall, green and grey roofs may contribute significantly to stormwater management during winter months; however, careful consideration of winter events must be taken into account when designing green and grey roofs in cold climate regions.

#### CRedit authorship contribution statement

**Noëlie Maurin:** Writing – original draft, Visualization, Software, Methodology, Formal analysis, Conceptualization. **Elhadi H.M. Abdalla:** Writing – original draft, Visualization, Software, Methodology,

Formal analysis, Conceptualization. **Tone Merete Muthanna:** Writing – review & editing, Supervision, Methodology, Conceptualization. **Edvard Sivertsen:** Writing – review & editing, Supervision, Methodology, Conceptualization.

#### Declaration of competing interest

The authors declare that they have no known competing financial interests or personal relationships that could have appeared to influence the work reported in this paper.

#### Data availability

Data will be made available on request.

#### Acknowledgments

The study was part of the Klima 2050 project (grant no. 237859/030) which was financed by the Research Council of Norway and the project partners.

#### Appendix A. Supplementary data

Supplementary data to this article can be found online at <https://doi.org/10.1016/j.scitotenv.2024.174132>.

#### References

- Abdalla, E., Alfredsen, K., Merete Muthanna, T., 2022. Towards improving the calibration practice of conceptual hydrological models of extensive green roofs. *J. Hydrol.* 607, 127548 <https://doi.org/10.1016/j.jhydrol.2022.127548>.
- Abdalla, E.M.H., Pons, V., Stovin, V., De-Ville, S., Fassman-Beck, E., Alfredsen, K., Muthanna, T.M., 2021. Evaluating different machine learning methods to simulate runoff from extensive green roofs. *Hydrol. Earth Syst. Sci.* 25, 5917–5935. <https://doi.org/10.5194/hess-25-5917-2021>.
- Almorox, J., Quej, V.H., Martí, P., 2015. Global performance ranking of temperature-based approaches for evapotranspiration estimation considering Köppen climate classes. *J. Hydrol.* 528, 514–522. <https://doi.org/10.1016/j.jhydrol.2015.06.057>.
- Andradóttir, H.Ó., Arnardóttir, A.R., Zaqout, T., 2021. Rain on snow induced urban floods in cold maritime climate: risk, indicators and trends. *Hydrol. Process.* 35 <https://doi.org/10.1002/hyp.14298>.
- Bengtsson, L., Grahm, L., Olsson, J., 2005. Hydrological function of a thin extensive green roof in southern Sweden. *Hydrol. Res.* 36, 259–268. <https://doi.org/10.2166/nh.2005.0019>.
- Bergström, S., Forsman, A., 1973. Development of a conceptual deterministic rainfall-runoff model. *Hydrol. Res.* 4, 147–170. <https://doi.org/10.2166/nh.1973.0012>.
- Bevilacqua, P., 2021. The effectiveness of green roofs in reducing building energy consumptions across different climates. A summary of literature results. *Renew. Sustain. Energy Rev.* 151, 111523 <https://doi.org/10.1016/j.rser.2021.111523>.
- Bosco, C., Abdalla, Elhadi Mohsen Hassan, Muthanna, T.M., Alfredsen, K., Rasten, B., Kjennbakken, H., Sivertsen, E., 2023. Evaluating the Stormwater management model for hydrological simulation of infiltration swales in cold climates. *Blue-Green Syst.* 5, 306–320. <https://doi.org/10.2166/bgs.2023.044>.
- Braskerud, B.C., Paus, K.H., 2022. Retention of snowmelt and rain from extensive green roofs during snow-covered periods. *Blue-Green Syst.* 4, 184–196. <https://doi.org/10.2166/bgs.2022.011>.
- Chen, X., Long, D., Hong, Y., Zeng, C., Yan, D., 2017. Improved modeling of snow and glacier melting by a progressive two-stage calibration strategy with GRACE and multisource data: how snow and glacier meltwater contributes to the runoff of the Upper Brahmaputra River basin? *Water Resour. Res.* 53, 2431–2466. <https://doi.org/10.1002/2016WR019656>.
- Gupta, H.V., Kling, H., Yilmaz, K.K., Martinez, G.F., 2009. Decomposition of the mean squared error and NSE performance criteria: implications for improving hydrological modelling. *J. Hydrol.* 377, 80–91. <https://doi.org/10.1016/j.jhydrol.2009.08.003>.
- Hall, P., Keilegom, I.V., 2003. Using difference-based methods for inference in nonparametric regression with time series errors. *J. R. Stat. Soc. Ser. B Stat. Methodol.* 65, 443–456. <https://doi.org/10.1111/1467-9868.00395>.
- Hamouz, V., Muthanna, T.M., 2019. Hydrological modelling of green and grey roofs in cold climate with the SWMM model. *J. Environ. Manage.* 249, 109350 <https://doi.org/10.1016/j.jenvman.2019.109350>.
- Hamouz, V., Lohne, J., Wood, J., Muthanna, T., 2018. Hydrological performance of LECA-based roofs in cold climates. *Water* 10, 263. <https://doi.org/10.3390/w10030263>.
- Johannessen, B., Muthanna, T., Braskerud, B., 2018. Detention and retention behavior of four extensive green roofs in three Nordic climate zones. *Water* 10, 671. <https://doi.org/10.3390/w10060671>.

- Jungels, J., Rakow, D.A., Allred, S.B., Skelly, S.M., 2013. Attitudes and aesthetic reactions toward green roofs in the northeastern United States. *Landsc. Urban Plan.* 117, 13–21. <https://doi.org/10.1016/j.landurbplan.2013.04.013>.
- Krasnogorskaya, N., Longobardi, A., Mobilia, M., Khasanova, L., Shchelchkova, A., 2019. Hydrological modeling of green roofs runoff by Nash Cascade model. *Open Civ. Eng. J.* 13, 163–171. <https://doi.org/10.2174/1874149501913010163>.
- Kratky, H., Li, Z., Chen, Y., Wang, C., Li, X., Yu, T., 2017. A critical literature review of bioretention research for stormwater management in cold climate and future research recommendations. *Front. Environ. Sci. Eng.* 11, 16. <https://doi.org/10.1007/s11783-017-0982-y>.
- Li, D., Lettenmaier, D.P., Margulis, S.A., Andreadis, K., 2019. The role of rain-on-snow in flooding over the conterminous United States. *Water Resour. Res.* 55, 8492–8513. <https://doi.org/10.1029/2019WR024950>.
- Lind, P., Belušić, D., Médus, E., Dobler, A., Pedersen, R.A., Wang, F., Matte, D., Kjellström, E., Landgren, O., Lindstedt, D., Christensen, O.B., Christensen, J.H., 2023. Climate change information over Fennoscandinavia produced with a convection-permitting climate model. *Climate Dynam.* 61, 519–541. <https://doi.org/10.1007/s00382-022-06589-3>.
- Lindström, G., Johansson, B., Persson, M., Gardelin, M., Bergström, S., 1997. Development and test of the distributed HBV-96 hydrological model. *J. Hydrol.* 201, 272–288. [https://doi.org/10.1016/S0022-1694\(97\)00041-3](https://doi.org/10.1016/S0022-1694(97)00041-3).
- Mullen, K.M., Ardia, D., Gil, D.L., Windover, D., Cline, J., 2011. DEoptim: an R package for global optimization by differential evolution. *J. Stat. Softw.* 40, 1–26. <https://doi.org/10.18637/jss.v040.i06>.
- Nash, J.E., Sutcliffe, J.V., 1970. River flow forecasting through conceptual models part I — a discussion of principles. *J. Hydrol.* 10, 282–290. [https://doi.org/10.1016/0022-1694\(70\)90255-6](https://doi.org/10.1016/0022-1694(70)90255-6).
- Oudin, L., Hervieu, F., Michel, C., Perrin, C., Andréassian, V., Anctil, F., Loumagne, C., 2005. Which potential evapotranspiration input for a lumped rainfall-runoff model?: part 2—towards a simple and efficient potential evapotranspiration model for rainfall-runoff modelling. *J. Hydrol.* 303, 290–306. <https://doi.org/10.1016/j.jhydrol.2004.08.026>.
- Palla, A., Sansalone, J.J., Gnecco, I., Lanza, L.G., 2011. Storm water infiltration in a monitored green roof for hydrologic restoration. *Water Sci. Technol. J. Int. Assoc. Water Pollut. Res.* 64, 766–773. <https://doi.org/10.2166/wst.2011.171>.
- Palla, A., Gnecco, I., Lanza, L.G., 2012. Compared performance of a conceptual and a mechanistic hydrologic models of a green roof. *Hydrol. Process.* 26, 73–84. <https://doi.org/10.1002/hyp.8112>.
- Pons, V., Muthanna, T.M., Sivertsen, E., Bertrand-Krajewski, J.-L., 2022. Revising green roof design methods with downscaling model of rainfall time series. *Water Sci. Technol.* 85, 1363–1371. <https://doi.org/10.2166/wst.2022.023>.
- Santos, M.L., Silva, C.M., Ferreira, F., Matos, J.S., 2023. Hydrological analysis of green roofs performance under a Mediterranean climate: a case study in Lisbon. *Portugal. Sustainability* 15, 1064. <https://doi.org/10.3390/su15021064>.
- Seibert, J., 1997. Estimation of parameter uncertainty in the HBV model: paper presented at the Nordic hydrological conference (Akureyri, Iceland - august 1996). *Hydrol. Res.* 28, 247–262. <https://doi.org/10.2166/nh.1998.15>.
- Seibert, J., Bergström, S., 2022. A retrospective on hydrological catchment modelling based on half a century with the HBV model. *Hydrol. Earth Syst. Sci.* 26, 1371–1388. <https://doi.org/10.5194/hess-26-1371-2022>.
- Sezen, C., Šraj, M., Medved, A., Bezak, N., 2020. Investigation of rain-on-snow floods under climate change. *Appl. Sci.* 10, 1242. <https://doi.org/10.3390/app10041242>.
- Shafique, M., Kim, R., Rafiq, M., 2018. Green roof benefits, opportunities and challenges — a review. *Renew. Sustain. Energy Rev.* 90, 757–773. <https://doi.org/10.1016/j.rser.2018.04.006>.
- She, N., Pang, J., 2010. Physically based green roof model. *J. Hydrol. Eng.* 15, 458–464. [https://doi.org/10.1061/\(ASCE\)HE.1943-5584.0000138](https://doi.org/10.1061/(ASCE)HE.1943-5584.0000138).
- Sims, A.W., Robinson, C.E., Smart, C.C., Voegt, J.A., Hay, G.J., Lundholm, J.T., Powers, B., O'Carroll, D.M., 2016. Retention performance of green roofs in three different climate regions. *J. Hydrol.* 542, 115–124. <https://doi.org/10.1016/j.jhydrol.2016.08.055>.
- Soulis, K.X., Valiantzas, J.D., Ntoulas, N., Kargas, G., Nektarios, P.A., 2017. Simulation of green roof runoff under different substrate depths and vegetation covers by coupling a simple conceptual and a physically based hydrological model. *J. Environ. Manage.* 200, 434–445. <https://doi.org/10.1016/j.jenvman.2017.06.012>.
- Stovin, V., 2010. The potential of green roofs to manage urban Stormwater. *Water Environ. J.* 24, 192–199. <https://doi.org/10.1111/j.1747-6593.2009.00174.x>.
- Stovin, V., Vesuviano, G., Kasmin, H., 2012. The hydrological performance of a green roof test bed under UK climatic conditions. *J. Hydrol.* 414–415, 148–161. <https://doi.org/10.1016/j.jhydrol.2011.10.022>.
- Stovin, V., Poë, S., Berretta, C., 2013. A modelling study of long term green roof retention performance. *J. Environ. Manage.* 131, 206–215. <https://doi.org/10.1016/j.jenvman.2013.09.026>.
- Stovin, V., Vesuviano, G., De-Ville, S., 2017. Defining green roof detention performance. *Urban Water J.* 14, 574–588. <https://doi.org/10.1080/1573062X.2015.1049279>.
- Susca, T., Gaffin, S.R., Dell'Osso, G.R., 2011. Positive effects of vegetation: urban heat island and green roofs. *Environ. Pollut., selected papers from the conference urban environmental pollution: overcoming obstacles to sustainability and quality of life (UEP2010)*, 20–23 June 2010. Boston, USA 159, 2119–2126. <https://doi.org/10.1016/j.envpol.2011.03.007>.
- Thiemig, V., Rojas, R., Zambrano-Bigiarini, M., De Roo, A., 2013. Hydrological evaluation of satellite-based rainfall estimates over the Volta and Baro-Akobo Basin. *J. Hydrol.* 499, 324–338. <https://doi.org/10.1016/j.jhydrol.2013.07.012>.
- Vesuviano, G., Sonnenwald, F., Stovin, V., 2013. A two-stage storage routing model for green roof runoff detention. *Water Sci. Technol.* 69, 1191–1197. <https://doi.org/10.2166/wst.2013.808>.
- Vormoor, K., Lawrence, D., Schlichting, L., Wilson, D., Wong, W.K., 2016. Evidence for changes in the magnitude and frequency of observed rainfall vs. snowmelt driven floods in Norway. *J. Hydrol.* 538, 33–48. <https://doi.org/10.1016/j.jhydrol.2016.03.066>.
- Wooster, E.I.F., Fleck, R., Torpy, F., Ramp, D., Irga, P.J., 2022. Urban green roofs promote metropolitan biodiversity: a comparative case study. *Build. Environ.* 207, 108458. <https://doi.org/10.1016/j.buildenv.2021.108458>.
- Yang, D., Elomaa, E., Tuominen, A., Aaltonen, A., Goodison, B., Gunther, T., Golubev, V., Sevruck, B., Madsen, H., Milkovic, J., 1999. Wind-induced precipitation Undercatch of the Hellmann gauges. *Hydrol. Res.* 30, 57–80. <https://doi.org/10.2166/nh.1999.0004>.
- Yin, H., Kong, F., Dronova, I., 2019. Hydrological performance of extensive green roofs in response to different rain events in a subtropical monsoon climate. *Landsc. Ecol. Eng.* 15, 297–313. <https://doi.org/10.1007/s11355-019-00380-z>.
- Zaqout, T., Andradóttir, H.O., Sörensen, J., 2023. Trends in soil frost formation in a warming maritime climate and the impacts on urban flood risk. *J. Hydrol.* 617, 128978. <https://doi.org/10.1016/j.jhydrol.2022.128978>.
- Zhang, S., Lin, Z., Sunxun, Z., Ge, D., 2021. Stormwater retention and detention performance of green roofs with different substrates: observational data and hydrological simulations. *J. Environ. Manage.* 291, 112682. <https://doi.org/10.1016/j.jenvman.2021.112682>.